JOURNAL OF SOLID STATE CHEMISTRY 86, 41–49 (1990)

Transition Orthorhombic ↔ Rutile in $xMFeO_4$-$(1-x)ZnF_2$ Phases (M = Ta, Nb and $x > 0.7$)

G. POURROY, E. LUTANIE, AND P. POIX

IPCMS, Groupe de Chimie des Matériaux Inorganiques, UM380046 EHICS, 1 rue Blaise Pascal BP296, 67008 Strasbourg Cedex, France

Received July 7, 1989; in revised form December 5, 1989

$xMFeO_4$-$(1-x)ZnF_2$ solid solutions with M = Ta, Nb are synthesized and studied by means of X-ray diffraction measurements. They exist only in the limited domain $x \geq 0.75$. Niobium compounds always present an orthorhombic structure of α-PbO_2 type while tantalum phases have a rutile structure above 700°C and the orthorhombic structure at lower temperatures. For the orthorhombic phases $x = 0.9$, a surstructure of wolframite type appears. Tantalum orthorhombic phase $x = 0.9$ has a ferrimagnetic behavior under 150 K. The others exhibit antiferromagnetism. © 1990 Academic Press, Inc.

Introduction

A phase transition between rutile (space group $P4_2/mnm$) and orthorhombic structures of α-PbO_2 type (space group $Pbcn$) is often encountered in oxides and fluorides of transition metals (*1*). Rutile structure is obtained at high temperature and normal pressure, and orthorhombic at lower temperature or under pressure (*2*). For instance, $NbFeO_4$ is rutile above 1380°C, and of α-PbO_2 type (ixiolite) between 1085 and 1380°C. At lower temperature, the wolframite structure (space group $P2/c$), which is an ordered form of the previous orthorhombic structure, is observed (*3, 4*). In this structural transition, the chains of MO_6 octahedra, straight along the c axis of the rutile, are staggered along the a axis in the α-PbO_2 structure (Fig. 1). Such transformations may occur by the movement of cation in adjoining layers along the edge of an octahedron to a previously unoccupied site (*2*).

The cations involved also have a preponderant role. Nb^{5+}, Fe^{3+}, Mn^{2+}, or Zn^{2+} prefer α-PbO_2 structure while Ta^{5+}, Ni^{2+}, and V^{3+} the rutile arrangement. For instance, $TaFeO_4$ is rutile in the temperature range for which $NbFeO_4$ is orthorhombic (*5*). $MnTa_2O_6$ and $ZnTa_2O_6$ have a columbite structure, surstructure of α-PbO_2, while $NiTa_2O_6$ presents the trirutile structure (*6–8*).

Cationic preference for one structure or other was recently observed in solid solutions between $TaMO_4$ (M = Fe, V) and $M'F_2$ (M' = Ni, Mn) (*9, 10*). Nickel compounds $TaMNiO_4F_2$ (M = Fe, V) were found to crystallize in the rutile structure at 650 and 700°C, respectively. The latter transforms partly into an orthorhombic structure of α-PbO_2 type at 550°C for $TaFeNiO_4F_2$.

The solid solution $xTaMO_4$-$(1-x)MnF_2$ (M = Fe, V) exists in a limited domain ($x >$ 0.85). The orthorhombic form is easily obtained for M = Fe at 720°C and transforms

0022-4596/90 $3.00
Copyright © 1990 by Academic Press, Inc.
All rights of reproduction in any form reserved.

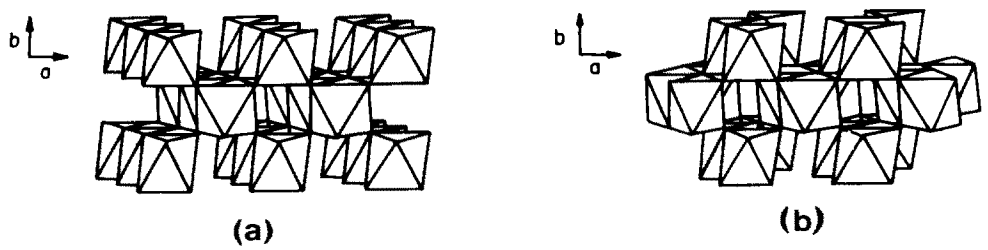

FIG. 1. Schematic representation of crystallographic cells for rutile (a) and α-PbO_2 (b) structures.

into rutile above 750°C. In the vanadium case, the rutile structure is always observed, but an accurate study of lines shape in the diffraction pattern indicates that the structure is not very pure rutile below 850°C. These observations allow us to conclude that Ni^{2+} and V^{3+} favor more the rutile structure than do Mn^{2+} and Fe^{3+}, respectively. Furthermore, this transformation goes with a change of magnetic properties. The orthorhombic phase exhibits ferrimagnetism at 6 K probably generated by a cationic order between Ta^{5+} on one hand and Mn^{2+} and Fe^{3+} on the other hand. This order can be partial, so it would be interesting to synthesize similar solid solutions. Following the structural studies of $NbFeO_4$ and $TaFeO_4$, we can expect an increase of the ordering by substituting Ta^{5+} for Nb^{5+}. The ferrimagnetism can be altered by replacing Mn^{2+} by Zn^{2+}. So we study here the structural and magnetic properties of the solid solutions $xMFeO_4$-$(1 - x)ZnF_2$ ($M = Nb^{5+}$, Ta^{5+}).

Experimental

Solid solutions between $MFeO_4$ (M = Nb, Ta) and ZnF_2 are prepared using the starting compounds ZnF_2, M_2O_5 (M = Nb, Ta) and Fe_2O_3. ZnF_2 is synthesized from ZnO and NH_4F using an original routine already described elsewhere (*11*). For the synthesis of the oxides M_2O_5 (M = Nb, Ta), the chlorides MCl_5 are first dissolved in anhydrous alcohol. The resulting solution is stirred while NH_4OH is added, giving thus a white precipitate of tantalum or niobium hydroxide. A powder of well-crystallized M_2O_5 (M = Nb, Ta) is obtained at 700°C. Iron oxide, Fe_2O_3, is synthesized by decomposition of iron(II) oxalate at 750°C.

The so obtained tantalum (or niobium) and iron oxides, taken in a stoichiometric ratio, are ground together in dried alcohol for 1 hr. This suspension is then heated up to 120°C until all alcohol is eliminated, then up to 1000°C for half an hour. This treatment eliminates traces of water, which sometimes cause the formation of impurities such as MO_2F (M = Nb, Ta) in the final compound. ZnF_2 is then added to the mixture Fe_2O_3-M_2O_5 (M = Nb, Ta). After grinding, the powder is put into a gold crucible and introduced into an inconel tube. The whole is heated under dried argon. The different thermal treatments are listed in Table I. The second heating is followed by a rapid cooling down to room temperature for the thermal treatments C and E.

$TaFeO_4$ and $NbFeO_4$ are prepared by heating the mixture Fe_2O_3-M_2O_5 (M = Nb, Ta) at 1000°C. Three annealings of one day separated by grindings are necessary to eliminate traces of M_2O_5 and Fe_2O_3.

The samples are studied by means of X-ray diffraction and magnetic measurements. X-ray powder diffraction patterns have been taken using a Kristalloflex Siemens diffractometer and cobalt radiation. Al_2O_3 has been used as internal standard for measuring diffraction angles. Mag-

TABLE I

CHARACTERISTICS OF THE SOLID SOLUTIONS $M_xFe_xZn_{1-x}O_{4x}F_{2(1-x)}$ (M = Nb, Ta): THERMAL TREATMENTS, STRUCTURES, AND COLORS

M	Ta			Nb	
x =	0.75, 0.8	0.9	0.75, 0.8, 0.9	0.75, 0.8, 0.9	
Treatment	A	B	C	D	E
First heating	700°C–50 hr	700°C–50 hr	700°C–50 hr	700°C–50 hr	700°C–50 hr
Second heating	650°C–50 hr	650°C–50 hr	850°C–½ hr		920°C–1 hr
Quenching			Yes		Yes
Structure	Orthorhomic + rutile	Orthorhomic	Rutile	Orthorhomic	Orthorhomic + rutile + $ZnFe_2O_4$
Color	Yellow-brown	Yellow-brown	Brown	Red-brown	Black

netic susceptibility measurements were performed with a pendulum-type magnetometer in the temperature range 4.2–300 K and magnetization measurements using a magnetometer designed in our laboratory.

General Characteristics of the Solid Solutions $M_xFe_xZn_{1-x}O_{4x}F_{2(1-x)}$ (M = Nb, Ta)

As previously observed in the system xTaFeO$_4$-(1 − x)MnF$_2$ (*10*), the reaction temperature strongly decreases when some metal bifluoride, ZnF_2 in our case, is added to the mixture M_2O_5-Fe_2O_3 (M = Nb, Ta). Indeed, the latter gives $MFeO_4$ (M = Nb, Ta) above 1000°C and the oxyfluoride reported here, $x < 0.9$, are completely formed at 700°C, after an annealing of 50 hr. For $x > 0.9$, the reaction temperature is higher because x is close to 1: a complete reaction is not observed at 700°C for $x = 0.95$. This reaction temperature drop is assigned to the formation of TaF_5 as an intermediate compound, its volatility making the total synthesis easier.

The solid solution is first studied for different x values. X-ray diffraction measurements show that M_2O_5 (M = Nb, Ta) and Fe_2O_3 always disappear, whatever x may be, even though ZnF_2 is detected when $x < 0.7$. So, to be sure that some ZnF_2 is not present in our samples, we focus our study on the solid solutions $x = 0.9$, 0.8, and 0.75.

The low temperature tantalum phases, resulting from the thermal treatments A and B, present on orthorhombic structure of α-PbO_2 type, isomorphous of $NbFeO_4$ and the orthorhombic $Ta_{.9}Fe_{.9}Mn_{.1}O_{3.6}F_{.2}$ phase when $x = 0.9$ and of the low temperature phase of $TaFeNiO_4F_2$ when $x = 0.8$ and 0.75 (*9*, *10*). Nevertheless, the most intense reflections of a rutile structure appear in the patterns after heating at 700°C. The second annealing at 650°C allow them to disappear when $x = 0.9$. Below 630°C, some Fe_2O_3 is thrown out.

Accordingly, pure rutile tantalum phases can be obtained by long annealings above 700°C. But, they are more rapidly synthesized by heating the powders at 850°C for half an hour (thermal treatment C) and quenching them down to room temperature.

The transition orthorhombic → rutile is much more difficult to observe in the niobium phases. Weak reflections of rutile structure appear in the X-ray diffraction patterns of samples heated up to 920°C. Furthermore, the compounds decompose,

TABLE II

CELL PARAMETERS AND VOLUMES OF ORTHOMBIC AND RUTILE PHASES $M_xFe_xZn_{1-x}O_{4x}F_{2(1-x)}$ (M = Nb, Ta)

Compound	x	Structure	a (Å)	b (Å)	c (Å)	V (Å^3)
$Ta_xFe_xZn_{1-x}O_{4x}F_{2(1-x)}$	0.9	Orthorhombic	4.64_9	5.59_5	5.03_1	130.9
	0.8	Orthorhombic	4.65_2	5.61_3	5.03_5	131.5
	0.75	Orthorhombic	4.65_6	5.61_4	5.03_8	131.7
	1.	Rutile	4.68_2		3.04_8	66.8
	0.9	Rutile	4.68_3		3.05_2	66.9
	0.8	Rutile	4.68_5		3.05_8	67.1
	0.75	Rutile	4.68_7		3.06_1	67.2
$Nb_xFe_xZn_{1-x}O_{4x}F_{2(1-x)}$	1.	Orthorhombic	4.64_7	5.61_3	5.00_5	130.5
	0.9	Orthorhombic	4.65_2	5.62_5	5.00_7	131.0
	0.8	Orthorhombic	4.66_0	5.63_1	5.01_9	131.7
	0.75	Orthorhombic	4.66_2	5.63_6	5.02_1	131.9

giving thus $ZnFe_2O_4$ and probably TaF_5 which evolves. So, no studies have been performed on the rutile niobium phases.

Crystallographic Study of Rutile $Ta_xFe_xZn_{1-x}O_{4x}F_{2(1-x)}$ (x = 0.75, 0.8, and 0.9)

Powder diffraction patterns of the tantalum phases submitted to the thermal treatment C indicate that they crystallize in the rutile structure (space group $P4_2/mnm$). Their cell parameters are listed in Table II, in addition to the $TaFeO_4$ ones (*12*). Intensities of the diffraction lines were measured for the sample x = 0.75. Its lattice spacings and their corresponding intensities are reported in Table III. The intensities have been computed assuming a statistical occupation of the metallic sites (2a) and a mean positional parameter u for the anions in site 4f. A distinction between the anionic sites has not been taken into account since it does not modify the intensities to a great extent. The very weak 120 diffraction line has been eliminated from the calculation. The better agreement between the experimental and calculated intensities of diffraction lines is given by the smallest reliability factor $R = \Sigma|I_{calc} - I_{obs}|/\Sigma I_{obs}$. The smallest value R = 5.2% has been obtained with u = 0.293.

Intensities of samples heated at higher temperatures (900–950°C) for half an hour do not fit the theoretical values. No other phases appear. Nevertheless, it indicates that the compound is no more preserved.

Crystallographic Studies of the Orthorhombic Phases $M_xFe_xZn_{1-x}O_{4x}F_{2(1-x)}$ (x = 0.75, 0.8, 0.9 and M = Nb, Ta)

Powder diffraction patterns of phases x = 0.75, 0.8, and 0.9, submitted to the thermal treatment A, B, or D, were recorded (Table I). A unique orthorhombic phase of α-PbO_2 type is observed for niobium and x = 0.9 tantalum phases, while the most intense reflections of rutile phase are detected in the tantalum phases x = 0.8 and 0.75. As the cristallographic parameters correspond to the pure rutile phases x = 0.8 and 0.75, the orthorhombic phase has the expected chemical formula. Cell parameters of all orthorhombic compounds are reported in Table II.

The lattice spacings of $Ta_{.9}Fe_{.9}Zn_{.1}O_{3.6}F_{.2}$

TABLE III

EXPERIMENTAL AND CALCULATED LATTICE SPACINGS AND INTENSITIES OF THE RUTILE PHASE $Ta_{.75}Fe_{.75}Zn_{.25}O_3F_{.5}$ (SPACE GROUP $P4_2/mnm$)

hkl	d_{obs}	I_{obs}	d_{calc}	I_{calc}
110	3.314	100	3.314	100
101	2.565	81	2.563	79
200	2.344	20	2.344	20
111	2.249	6	2.249	4
120	2.097	<1	2.096	<1
121	1.730	61	1.730	57
220	1.658	16	1.657	15
002	1.531	7	1.531	6
130	1.483	12	1.482	13
301	1.391	30	1.390	12
112			1.392	15
202	1.282	6	1.281	6
231	1.196	12	1.196	12
400	1.172	4	1.172	4
222	1.125	8	1.124	8
330	1.105	4	1.105	4
141	1.065	25	1.066	11
132	1.066		1.065	12
240	1.0480	6	1.0480	6
103	0.9970	7	0.9970	6
402	0.9309	13	0.9304	11

and their corresponding intensities are reported in Table IV. This diffraction pattern, as well as that of $Nb_{.9}Fe_{.9}Zn_{.1}O_{3.6}F_{.2}$, is similar to the $NbFeO_4$ one; i.e., the reflections 100 and 011 forbidden in the α-PbO_2 structure are not zero in our case. The latter disappear in the diffraction patterns of the niobium phase $x = 0.8$ or 0.75, isomorphous of α-PbO_2. As their intensities are very weak, these reflections have been eliminated from the computations. The intensities of the samples $Ta_{.9}Fe_{.9}Zn_{.1}O_{3.6}F_{.2}$

TABLE IV

EXPERIMENTAL AND CALCULATED LATTICE SPACINGS AND INTENSITIES OF THE ORTHORHOMBIC PHASE $Ta_{.9}Fe_{.9}Zn_{.1}O_{3.6}F_{.2}$ (SPACE GROUP *Pbcn*)

hkl	d_{obs}	I_{obs}	d_{calc}	I_{calc}
100	4.63	2	4.65	0
011	3.734	1	3.741	0
110	3.573	30	3.576	29
111	2.910	100	2.915	100
020	2.809	8	2.810	8
002	2.513	17	2.516	17
021	2.448	19	2.445	18
200	2.322	10	2.325	9
102	2.209	3	2.213	2
121	2.168	5	2.164	3

TABLE IV—*Continued*

hkl	d_{obs}	I_{obs}	d_{calc}	I_{calc}
112	2.056	10	2.058	10
022	1.872	6	1.871	6
220	1.789	6	1.788	5
130	1.734	65	1.731	13
202	1.705		1.707	15
221	1.685		1.685	21
113	1.519	14	1.518	14
310	1.493	1	1.494	1
222	1.457	42	1.457	4
023	1.437		1.438	7
311	1.429		1.432	11
132	1.429		1.426	13
040	1.403	1	1.399	1
041	1.351	6	1.348	5
302	1.318	<1	1.319	<1
321	1.309	<1	1.309	<1
312	1.283	3	1.284	2
004	1.256	3	1.258	2
223	1.223	4	1.223	4
330	1.193	6	1.192	4
114	1.185		1.187	2
241	1.169	10	1.166	6
400	1.162		1.162	2
024	1.147	1	1.147	1
313	1.115	23	1.115	5
204	1.105		1.106	4
150	1.092		1.088	1
242	1.084		1.082	1
332	1.078		1.077	7
043	1.074		1.074	3
420	1.074		1.073	1
151	1.067	4	1.063	4
402	1.055	7	1.055	3
421	1.048		1.050	4
224	1.0287	2	1.0287	2
134	1.0187	8	1.0175	7
152	1.008	3	0.9986	3
422	0.9875	11	0.9873	3
243	0.9768		0.9751	8
115	0.9679	5	0.9686	7
314	0.9615	2	0.9621	2

TABLE V

POSITIONAL PARAMETERS AND RELIABILITY FACTOR R FOR THE $Ta_{.9}Fe_{.9}Zn_{.1}O_{3.6}F_{.2}$ AND $Nb_{.75}Fe_{.75}Zn_{.25}O_3F_{.5}$ COMPOUNDS

	$Ta_{.9}Fe_{.9}Zn_{.1}O_{3.6}F_{.2}$	$Nb_{.75}Fe_{.75}Zn_{.25}O_3F_{.5}$
Cations		
x	0.000	0.000
y	0.173	0.176
z	0.250	0.250
Anions		
x	0.275	0.275
y	0.391	0.367
z	0.410	0.404
R	9%	7.4%

and $Nb_{.75}Fe_{.75}Zn_{.25}O_3F_{.5}$ have been calculated assuming a statistical distribution of the cations and the anions on sites 4c and 8d, respectively. The smallest reliability factors $R = \Sigma|I_{calc} - I_{obs}|/\Sigma I_{obs}$ have been obtained for the positional parameters given in Table V.

Magnetic Properties

Magnetic studies have been performed on the orthorhombic $Ta_{.9}Fe_{.9}Zn_{.1}O_{3.6}F_{.2}$, the rutile tantalum, and orthorhombic niobium phases $x = 0.75$, 0.9, and 1. The raw susceptibility data are corrected from diamagnetism according to the Slater and Angus (*14*) method.

The most simple behaviors are encountered for the rutile tantalum phases. The variations of their susceptibilities versus temperature are presented in Fig. 2. One can note the shift of the susceptibility maximum toward low temperatures when ZnF_2 is added. It occurs at 12–13 K for $TaFeO_4$ ($x = 1$), 8–10 K, and under 4 K for $x = 1$. The slopes of straight lines $1/X = C/(T - \theta)$, taken above 200 K, correspond to Curie constants below theoretical values, indicating that the paramagnetic domain is still not reached (Table VI). Let us note that the

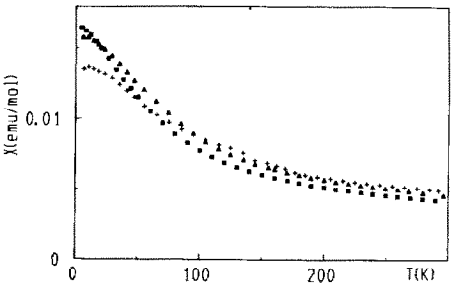

FIG. 2. Variation of inverse susceptibilities versus temperature for the rutile phases $Ta_xFe_xZn_{1-x}O_{4x}F_{2(1-x)}$ ($x = 0.75$(■), 0.9(▲), and 1(+)).

variation of susceptibility found for $TaFeO_4$ is in agreement with the results of Christenen *et al.* (*13*).

Niobium orthorhombic phases, despite the difference of structure, have similar behaviors. The susceptibility of $NbFeO_4$ ($x = 1$) exhibits a sharp maximum at 47 K which has almost completely disappeared when $x = 0.9$ (Fig. 3). The former follows a Curie–Weiss law $\chi = 4.18/(T + 89)$ above 200 K. The Curie constant is lower than the theoretical value, probably because the paramagnetic domain is not completely reached. The Curie constant values measured above 200 K strongly decrease when ZnF_2 is added, showing that the paramagnetic behavior occurs at higher temperatures in the oxyfluoride phases (Table VI).

TABLE VI

THEORETICAL CURIE CONSTANTS AND EXPERIMENTAL CURIE CONSTANTS AND WEISS TEMPERATURES FOR THE $Ta_xFe_xZn_{1-x}O_{4x}F_{2(1-x)}$ AND $Nb_xFe_xZn_{1-x}O_{4x}F_{2(1-x)}$ COMPOUNDS WITH $x = 1$, .9, .75

Compound	x	C_{th}	C_{exp}	θ
$Ta_xFe_xZn_{1-x}O_xF_{2(1-x)}$	1	4.375	3.08	334
Rutile	.9	3.938	2.23	223
Rutile	.75	3.281	2.19	229
$Nb_xFe_xZn_{1-x}O_xF_{2(1-x)}$	.1	4.375	4.18	89
Orthorhombic	.9	3.938	2.38	27
Orthorhombic	.75	3.281	1.9	97

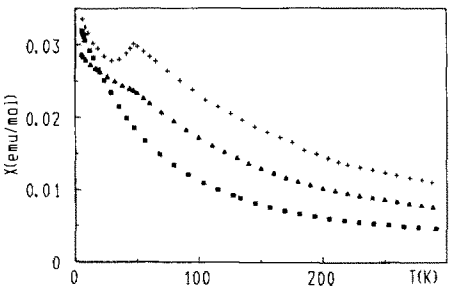

FIG. 3. Variation of inverse susceptibilities versus temperature for the orthorhombic phases $Nb_xFe_x Zn_{1-x}O_{4x}F_{2(1-x)}$ (x = 0.75(■), 0.9(▲), and 1(+)).

Magnetization measurements do not show any dependence toward magnetic field for niobium phases, unlike the tantalum orthorhombic compound. The latter is characterized by a maximum of magnetic moment XT at 95 K (Fig. 4). Magnetization measurements have been performed at different temperatures, 265, 150, 95, and 10 K. They are present in Fig. 5. A ferromagnetic component appears at 150 K. Its value increases when the temperature decreases. At 10 K, the compound $Ta_{.9}Fe_{.9}Zn_{.1}O_{3.6}F_{.2}$ is characterized by a coercive field of 1500G and a magnetic moment of 2.19 uem/g, i.e., 0.11 μ_B/mol at high magnetic field.

Discussion

Solid solutions $xMFeO_4$-$(1-x)ZnF_2$ with M = Nb, Ta exist in a limited domain,

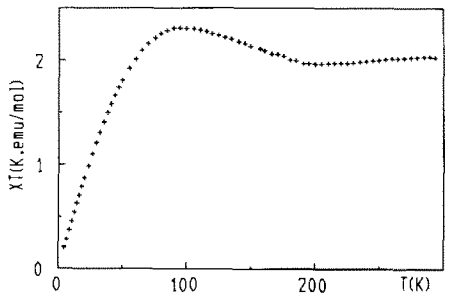

FIG. 4. Dependence of magnetization versus magnetic field for the orthorhombic phase $Ta_{.9}Fe_{.9}Zn_{.1}O_{3.6}F_{.2}$ at various temperatures.

$x \geq 0.75$, due to the difference of cationic sizes. Indeed, Nb^{5+}, Ta^{5+}, and Fe^{3+}, whose characteristic cation-oxygen lengths in an octahedral environment are 2.012, 2.016, and 2.02 Å, respectively, are smaller than Zn^{2+} (2.141 Å) (*15*). Nevertheless, the solubility domain is larger than in the manganese case for which $x > 0.85$ (*10*). The solid solutions present either an orthorhombic structure of α-PbO_2 type, or a rutile structure depending on the thermal treatments and the cations involved. The former is a low temperature phase encountered under 650 and 900 K for tantalum and niobium phases, respectively. Pure rutile structures are only obtained for tantalum phases above 700 K since these oxyfluoride phases decompose above 900 K giving MF_5 (M = Nb, Ta) which evolves and $ZnFeO_4$. Comparing the results to those previously obtained (*9*, *10*), we can conclude that Nb^{5+} and Mn^{2+} favor more the orthorhombic structure of α-PbO_2 type than do Ta^{5+} and Zn^{2+}.

Another parameter has an effect on the stability domain of one structure or other, the concentration of fluoride. The smaller x is, the lower the temperature of the phase transition. Slight addition of ZnF_2 seems to favor orthorhombic structure since $TaFeO_4$ becomes orthorhombic only under pressure (*16*). But the rutile domain is all the more spreaded toward the low temperatures because the concentration of ZnF_2 increases. Furthermore, the orthorhombic phases x = 0.9 seem to be more ordered. The diffraction lines 100 and 011, forbidden in the α-PbO_2 structure, appear when x = 0.9 and disappear when x decreases. They are present in the diffraction pattern of NbFeO_4, which crystallizes in the space group $P2/c$. This structure named wolframite is characterized by chains of Nb^{5+} separated by chains of Fe^{3+}. The addition of ZnF_2 breaks down this order. Because of the difference between oxidation degrees, Nb^{5+} or Ta^{5+} and Zn^{2+} cannot occupy the same

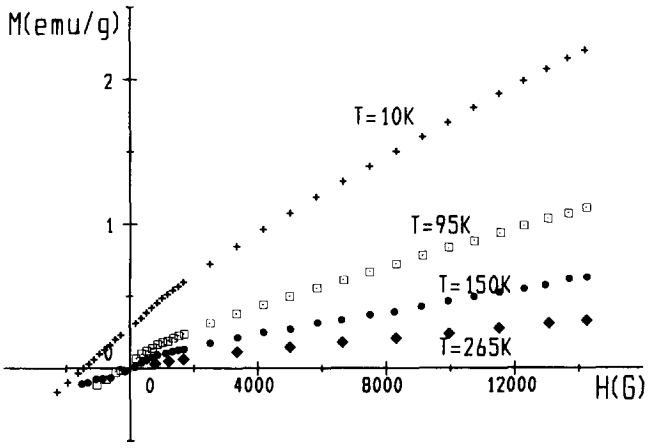

FIG. 5. Variation of magnetic moment versus magnetic field at different temperatures for the orthorhombic phase $Ta_{.9}Fe_{.9}Zn_{.1}O_{3.6}F_{.2}$.

crystallographic site. For low concentration of fluoride, one site is probably constituted from niobium (or tantalum) and a little of iron, and the other of iron and zinc. For increasing quantities of zinc, the difference of these sites toward the diffraction decreases.

The existence of two sublattices explains the behavior of the $Ta_{.9}Fe_{.9}Zn_{.1}O_{3.6}F_{.2}$ phase, similar to the corresponding manganese compound (*10*). Both are characterized by the same coercive field of about 1500G under 10 K. However, the saturation does not seem to be reached at this temperature.

Such a ferromagnetic component has not been observed for the niobium phase $x = 0.9$, although the latter presents an ordered structure of wolframite type. This can be brought together with the behaviors observed above 200 K. Indeed, magnetic interactions are stronger in $TaFeO_4$ than in $NbFeO_4$, since the Weiss temperatures, calculated for temperatures higher than 200 K, are greater in the tantalum case than in the niobium one (Table VI). This allows us to support that a coupling between the two sublattices occurs at lower temperatures in the niobium phase than in the tantalum compound, so that the tridimensional antiferromagnetism hides the effect of this coupling. This difference can be explained by a greater covalency of tantalum allowing an easier magnetic exchange between iron ions. Magnetic interactions are also strongly altered when ZnF_2 is added since the Curie constants of niobium phases calculated above 200 K are much smaller than is expected. Furthermore, the maximum observed for the curves $x = 1$ disappears in the temperature range 4.2–300 K and is probably shifted toward the low temperatures. In any case, numerous studies of similar phases with other cations such as V^{3+}, Cr^{3+}, and Fe^{3+} have to be performed to allow a final conclusion about these behaviors.

Acknowledgments

We thank A. Derory, IPCMS, GCMI, UM380046 EHICS, Strasbourg, for recording magnetization measurements.

References

1. Structure Reports 28, 72-13, 186-27, 477.
2. J. GALY AND S. ANDERSON, *J. Solid State Chem.* **3,** 525 (1971).

3. F. LAVES, G. BAYER, AND A. PANAGOS, *Schweiz. Mineral. Petrogr. Mitt.* **43,** 217 (1963).
4. R. S. ROTH AND J. L. WARING, *Amer. Mineral.* **49,** 242 (1964).
5. A. C. TURNOCK, *J. Amer. Ceram. Soc.* **48,** 258 (1965).
6. H. WEITZEL AND S. KLEIN, *Solid State Commun.* **12,** 113 (1973).
7. K. BRANDT, *Arkiv. Kemi. Mineral. Geol.* **17A,** No. 15 (1943).
8. A. BYSTRÖM, B. HOK, AND B. MASON, *Arkiv. Kemi. Mineral. Geol.* **15B,** No. 4 (1941).
9. G. POURROY, P. POIX, AND J. P. SANCHEZ, *J. Solid State Chem.* **74,** 27 (1988).
10. G. POURROY, P. POIX, AND S. MARIN, *J. Solid State Chem.* **81,** 112 (1989).
11. G. POURROY AND P. POIX, *J. Fluorine Chem.* **42,** 257 (1989).
12. M. GRILLET, Thèse 3e cycle Paris XI (1974).
13. A. CHRISTENEN, T. JOHANSSON, AND B. LEBECH, *J. Phys. C* **9,** 2601 (1976).
14. J. C. BERNIER AND P. POIX, *Actual. Chim.* **2,** 7 (1978).
15. P. POIX, *C. R. Acad. Sci.* **268,** 1139 (1969).
16. S. TAMURA, *Solid State Commun.* **12,** 597 (1973).